Local Analytical Solution for Compressible Turbulent Boundary Layers

L. Lakshminarayana*
Indian Institute of Science, Bangalore, India

An approximate local analysis is developed to solve the momentum integral equation, for internal or external, adiabatic or cooled, two-dimensional and axisymmetric compressible turbulent boundary-layer flows of air, using the power law for skin friction coefficient. A modified pressure-geometry parameter β is defined. Assuming local constancy for β, the momentum integral equation is solved analytically. The solution becomes exact for special cases of flow over a flat plate with arbitrary starting point of turbulent flow and fully developed flow over a cone. Some numerical examples are constructed to test the accuracy of the approximate local analysis and it is found that the calculated Stanton number is within about 3% of exact numerical solution.

Nomenclature

C = appears in Eq. (3)
C_f = skin friction coefficient (wall shear stress/$\frac{1}{2}\rho_e u_e^2$)
H = shape factor, $\int_0^\infty (1-\frac{\rho u}{\rho_e u_e})\,dy \Big/ \int_0^\infty \frac{\rho u}{\rho_e u_e}(1-\frac{u}{u_e})\,dy$
i = exponent of skin friction law, Eq. (3)
L = length of body; Fig. 1
M = Mach number
O = origin of x axis
r_w = normal distance of wall from axis
Re_x = Reynolds number based on x, $(\rho_e u_e x/\mu_e)$
Re_θ = Reynolds number based on θ, $(\rho_e u_e \theta/\mu_e)$
St = Stanton number, [wall heat flux/specific heat at constant pressure $\times \rho_e u_e (T_r - T_w)$]
t = starting point of turbulent flow, Fig. 1
T = temperature
T_{ref} = reference temperature, Eq. (21)
u = velocity tangential to wall
x = distance measured along body axis
$\bar{x}$ = defined by Eq. (4)
y = distance measured normal to wall
β = modified pressure-geometry parameter, Eq. (5)
γ = ratio of specific heats
ρ = density
σ = has value 0 or 1 respectively for two-dimensional or axisymmetric bodies
θ = momentum thickness, $\int_0^\infty \frac{\rho u}{\rho_e u_e}(1-\frac{u}{u_e})\,dy$
Φ = angle made by wall contour with x axis
μ = dynamic viscosity
ω = exponent of viscosity power law

Subscripts

c = cooled wall
e = boundary-layer edge
n = nth point in the interval of integration starting with point t as 1
o = stagnation
r = recovery
t = refers to the starting point of turbulent flow
w = wall
∞ = freestream
$o\infty$ = freestream stagnation

Received April 30, 1976; revision received Nov. 9, 1976.
Index categories: Boundary Layers and Convective Heat Transfer – Turbulent; Nozzle and Channel Flow; Launch Vehicle Systems (including Ground Support).

*Research Associate, Department of Aeronautical Engineering.

Introduction

THE momentum integral equation governing compressible turbulent boundary layers over two-dimensional and axisymmetric bodies[1] is nonlinear and no analytical solution exists. It is, therefore, usually solved by direct numerical integration. However, the direct numerical integration procedures are generally complex. For quick results, it would be of great value for a designer of aerospace systems to have a simple solution available in analytical form which, though approximate, has reasonable accuracy. An attempt is made in this paper to provide such a simple solution.

This paper contains general integral formulation of adiabatic or cooled compressible turbulent boundary layers. A local form of analytical solution is developed and described. The solution is shown to become exact for two special cases: boundary layer over a flat plate with arbitrary starting point of turbulent flow and fully turbulent boundary layer over a cone. Some numerical examples are solved to test the accuracy of the method.

Formulation

Consider the flow of air as shown in Fig. 1 in an external or internal boundary layer over a two-dimensional or axisymmetric body. The surface is adiabatic or cooled to any prescribed temperature T_c. The flow of interest here is the fully turbulent portion beyond t, the end point of transition.

The governing momentum integral equation[1] and boundary condition can be written as

$$\frac{d\theta}{dx} + \left[\frac{2-M_e^2+H}{M_e[1+(\gamma-1)/2M_e^2]}\frac{dM_e}{dx} + \frac{1}{r_w^\sigma}\frac{dr_w^\sigma}{dx}\right]\theta = (C_f/2)\sec\Phi \tag{1}$$

and

$$\theta(x_t) = \theta_t \tag{2}$$

$\sigma = 0$ or 1 depending upon whether the body is two-dimensional or axisymmetric. C_f and H are unknowns and the semiempirical form for the former is chosen to be proportional to power of Re_θ

$$C_f = C\,Re_\theta^{-i} \tag{3}$$

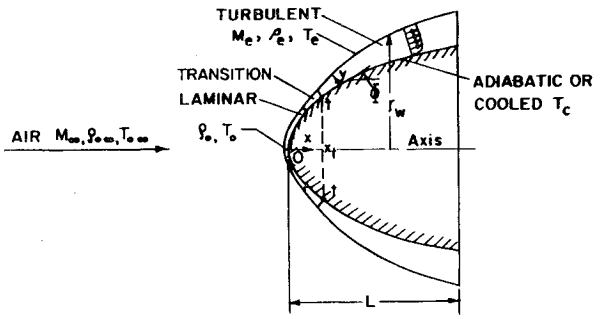

EXTERNAL BOUNDARY LAYER OVER A TWO-DIMENSIONAL OR AN AXISYMMETRIC BODY.

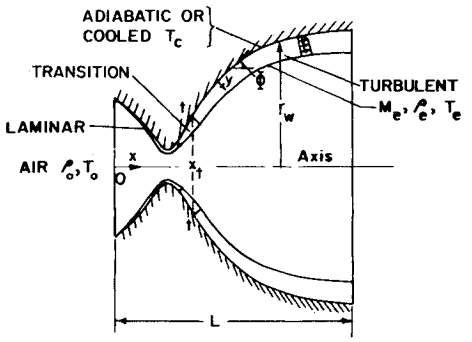

INTERNAL BOUNDARY LAYER OVER A TWO-DIMENSIONAL OR AN AXISYMMETRIC BODY.

Fig. 1 Physical model and coordinate system.

where C is a function of local properties, i is a constant usually having a range 0.2 to 0.25. H is also a function of local flow properties.

Several mathematical models appear in literature for C and H[2-4] and Spence's expressions[2] will be used.

Analysis

Introducing a new independent variable $\bar{x}$ such that

$$\bar{x}=\beta x \tag{4}$$

where,

$$\beta(x)=\Big[C\sec\Phi - \frac{\frac{\mu_e}{\rho_e u_e}\Big\{\frac{2-M_e^2+H}{M_e[1+(\gamma-1)/2M_e^2]}\frac{dM_e}{dx}+\frac{1}{r_w^a}\frac{dr_w^a}{dx}\Big\}}{\frac{1}{2}(C_f/C)^{(1+i)/i}}\Big] \cdot\Big(\frac{\rho_e u_e}{\mu_e}\Big)^{-i} \tag{5}$$

The numerator of the second term within the square brackets is a summation of two parts. The first part characterizes the pressure variation (through dM_e/dx) in the boundary layer. The second part characterizes the two-dimensional or axisymmetric geometry of the body. For a flat plate the second term becomes zero and β is therefore appropriately termed hereafter as "modified pressure-geometry parameter." Its dimensions are (length)^i.

Assuming β to be constant locally (i.e. derivative of β with respect to x to be negligible), Eq. (1) with the help of Eq. (3) reduces locally to

$$d\theta/d\bar{x}=\tfrac{1}{2}\theta^{-i} \tag{6}$$

This equation is easily integrable for θ at any point (or location) n in terms of its solution at the previous point $(n-1)$ and is given by

$$\theta_n=\Big(\frac{i+1}{2}\Big)^{1/(1+i)}\Big[\bar{x}_n-\bar{x}_{n-1}+\frac{2}{1+i}\theta_{n-1}^{i+1}\Big]^{1/(i+1)} \tag{7}$$

Returning to the original variable x, through Eq. (4), and remembering the assumption that β is constant locally, Eq. (7) becomes

$$\theta_n=\Big(\frac{i+1}{2}\Big)^{1/(1+i)}\Big[\beta_n(x_n-x_{n-1})+\frac{2}{i+1}\theta_{n-1}^{i+1}\Big]^{1/(i+1)} \tag{8}$$

Nondimensionalizing θ_n and x_n by $(\mu_e/\rho_e u_e)_n$, θ_{n-1} and x_{n-1} by $(\mu_e/\rho_e u_e)_{n-1}$, one gets

$$Re_{\theta_n}=\Big(\frac{i+1}{2}\Big)^{1/(i+1)}\Big[\beta_n\Big(\frac{\rho_e u_e}{\mu_e}\Big)_n^i\Big\{Re_{x_n} - \Big(\frac{\rho_e u_e}{\mu_e}\Big)_n\Big(\frac{\mu_e}{\rho_e u_e}\Big)_{n-1}\cdot Re_{x_{n-1}}\Big\}+\frac{2}{i+1}\Big\{\Big(\frac{\rho_e u_e}{\mu_e}\Big)_n \Big(\frac{\mu_e}{\rho_e u_e}\Big)_{n-1}\Big\}^{i+1} Re_{\theta_{n-1}}^{i+1}\Big]^{1/(i+1)} \tag{9}$$

C_{f_n} therefore, from Eq. (3), becomes

$$C_{f_n}=C_n\Big(\frac{i+1}{2}\Big)^{-1/(i+1)}\Big[\beta_n\Big(\frac{\rho_e u_e}{\mu_e}\Big)_n^i\Big\{Re_{x_n} - \Big(\frac{\rho_e u_e}{\mu_e}\Big)_n\Big(\frac{\mu_e}{\rho_e u_e}\Big)_{n-1}\cdot Re_{x_{n-1}}\Big\}+\frac{2}{i+1}\Big\{\Big(\frac{\rho_e u_e}{\mu_e}\Big)_n \cdot\Big(\frac{\mu_e}{\rho_e u_e}\Big)_{n-1}\Big\}^{i+1} Re_{\theta_{n-1}}^{i+1}\Big]^{-i/(i+1)} \tag{10}$$

It may be noticed, from Eq. (5), that β is a function of C_f. Substituting the value of β_n in Eq. (10) and simplifying yields

$$C_{f_n}=\Big(\frac{2}{1+i}\Big)^{i/(i+1)}C_n^{1/(1+i)} \Big[\Big(1+(1+i)\Big(\frac{\mu_e}{\rho_e u_e}\Big)_n\Big\{\frac{2-M_e^2+H}{M_e(1+(\gamma-1)/2M_e^2)}\frac{dM_e}{dx} + \frac{1}{r_w^a}\frac{dr_w^a}{dw}\Big\}\Big\{Re_{x_n} - \Big(\frac{\rho_e u_e}{\mu_e}\Big)_n\Big(\frac{\mu_e}{\rho_e u_e}\Big)_{n-1}Re_{x_{n-1}}\Big\}\Big)^{-1}\Big[\Big\{Re_{x_n} - \Big(\frac{\rho_e u_e}{\mu_e}\Big)_n\Big(\frac{\mu_e}{\rho_e u_e}\Big)_{n-1}Re_{x_{n-1}}\Big\}\sec\Phi_n+\frac{2}{(1+i)C_n} \cdot\Big\{\Big(\frac{\rho_e u_e}{\mu_e}\Big)_n\Big(\frac{\mu_e}{\rho_e u_e}\Big)_{n-1}\Big\}^{i+1} Re_{\theta_{n-1}}^{i+1}\Big]^{-1/(i+1)} \tag{11}$$

Replacing $Re_{\theta_{n-1}}$ in terms of $C_{f_{n-1}}$ from Eq. (3) results in

$$C_{f_n}=\Big(\frac{2}{1+i}\Big)^{i/(i+1)}C^{1/(1+i)} \Big[\Big(1+(1+i)\Big(\frac{\mu_e}{\rho_e u_e}\Big)_n\Big\{\frac{2-M_e^2+H}{M_e(1+(\gamma-1)/2M_e^2)}\frac{dM_e}{dx} + \frac{1}{r_w^a}\frac{dr_w^a}{dx}\Big\}\Big\{Re_{x_n} - \Big(\frac{\rho_e u_e}{\mu_e}\Big)_n\Big(\frac{\mu_e}{\rho_e u_e}\Big)_{n-1}Re_{x_{n-1}}\Big\}\Big)^{-1}$$

$$\cdot\left[\left\{Re_{x_n}-\left(\frac{\rho_e u_e}{\mu_e}\right)_n\left(\frac{\mu_e}{\rho_e u_e}\right)_{n-1}Re_{x_{n-1}}\right\}\sec\Phi_n + \frac{2}{(1+i)C_n}\left\{\left(\frac{\rho_e u_e}{\mu_e}\right)_n\left(\frac{\mu_e}{\rho_e u_e}\right)_{n-1}\right\}^{i+1}\left(\frac{C_{f_{n-1}}}{C_{n-1}}\right)^{-(1+i)/i}\right]^{-1/(i+1)} \tag{12}$$

Applying Eq. (12) repeatedly, C_f can now be evaluated at all points $n>2$. For $n=2$, C_{f_1} i.e., C_{f_t} is required and is obtained from Eqs. (3) and (2).

Exact Special Cases

Flat Plate with Arbitrary Starting Point of Turbulent Flow

For this case, $\Phi_n=\text{constant}=\Phi$, $[(1/r_w^a)(dr_w^a/dx)]_n=0$ and $(dM_e/dx)_n=0$. Further $(\rho_e u_e/\mu_e)_n=(\rho_e u_e/\mu_e)_{n-1}=\text{constant}=(\rho_e u_e/\mu_e)$. The surface is assumed to be isothermal or adiabatic.

Therefore $C_n=C_{n-1}=\text{constant}=C$ [see for instance, Eq. (19)]. Equation (12) hence reduces to

$$C_{f_n}=\left(\frac{2}{1+i}\right)^{i/(1+i)}C^{1/(1+i)}\left[(Re_{x_n}-Re_{x_{n-1}})\sec\Phi + \frac{2}{1+i}C^{1/i}C_{f_{n-1}}^{-(1+i)/i}\right]^{-i/(1+i)} \tag{13}$$

Equation (13) can be alternatively expressed as

$$C_f=\left(\frac{2}{1+i}\right)^{i/(1+i)}C^{1/(1+i)}\left[(Re_x-Re_{x_t})\sec\Phi + \frac{2}{1+i}C^{1/i}C_{f_t}^{-(1+i)/i}\right]^{-i/(1+i)} \tag{14}$$

This can be verified by evaluating C_{f_n} and $C_{f_{n-2}}$ from Eq. (14) and on substitution into Eq. (13) which would be identically satisfied. Further, Eq. (14) satisfies Eqs. (1) and (2). Thus the general local solution, Eq. (12), becomes exact for flow over a flat plate with the turbulent flow starting at an arbitrary point x_t and having skin friction C_{f_t}. This fact is to be expected because the local constancy approximation used for the modified pressure-geometry parameter in the general analysis becomes exact and attains a constant value $C(\rho_e u_e/\mu_e)^{-i}\sec\Phi$.

For fully developed flow, $x_t=0$, $\theta_t=0$, $C_{f_t}=\infty$ and $C_{f_t}^{-(1+i)/i}=0$. The skin friction coefficient, from Eq. (14), assumes

$$C_f=\left(\frac{2}{1+i}\right)^{i/(1+i)}C^{1/(1+i)}[Re_x\sec\Phi]^{-i/(1+i)} \tag{15}$$

Fully Turbulent Flow over a Cone

In this case $\Phi_n=\text{constant}=\Phi$ and $[(1/r_w^a)(dr_w^a/dx)]_n=1/x_n$. The flow is assumed to have freestream Mach number greater than one and the shock wave is assumed attached. Consequently $(dM_e/dx)_n=0$ and $(\rho_e u_e/\mu_e)_n=(\rho_e u_e/\mu_e)_{n-1}=\text{constant}=(\rho_e u_e/\mu_e)$. The surface is assumed isothermal or adiabatic. $C_n=C_{n-1}=\text{constant}=C$, similar to the case of flat plate. Equation (12) therefore becomes

$$C_{f_n}=\left(\frac{2}{1+i}\right)^{i/(1+i)}C^{1/(1+i)}\left(1+(1+i)\left(1-\frac{Re_{x_{n-1}}}{Re_{x_n}}\right)\right)^{-1}\cdot\left\{(Re_{x_n}-Re_{x_{n-1}})\sec\Phi+\frac{2}{1+i}C^{1/i}C_{f_{n-1}}^{(1+i)/i}\right\}^{-i/(i+1)} \tag{16}$$

Equation (16) can be shown, similar to Eq. (14), as equivalent to

$$C_f=[2/(1+i)]^{i/(1+i)}C^{1/(1+i)}[(2+i)^{-1}Re_x\sec\Phi]^{-i/(i+1)} \tag{17}$$

which also satisfies Eqs. (1) and (2). Equation (17) is thus another exact special solution of Eq. (12). β, as to be expected, attains a constant value $(2+i)^{-1}C(\rho_e u_e/\mu_e)^{-i}\sec\Phi$.

It may be noted here, on examining Eqs. (17) and (15), that the fully developed cone solution can be obtained from the fully developed flat plate solution if one replaces Re_x by $(2+i)^{-1}Re_x$. For $i=0.2$, proposed by Spence,[2] the multiplication factor, $(2+i)^{-1}$, becomes 0.4545. It is of interest to recall that Van Driest[5] obtained the multiplication factor as 0.5, very close to the present value, using universal laws derived from the mixing length hypothesis.

Numerical Examples

In this section three numerical examples are solved using the previous local analysis and an exact parabolic numerical technique.[6] For all the examples i, c and H are taken to be[2]

$$i=0.2 \tag{18}$$

$$C=0.0176\left(\frac{T_{\text{ref}}}{T_e}\right)^{-1+\omega i}\left(\frac{T_e}{T_0}\right)-\left(\frac{1}{\gamma-1}-\omega\right)i\left(\frac{\rho_0\mu_e}{\rho_e\mu_0}\right)^{-i} \tag{19}$$

and

$$H=-1+2.5\frac{T_w}{T_e}+\frac{T_r-T_w}{T_e} \tag{20}$$

where

$$T_{\text{ref}}=0.5(T_w+T_e)+0.22(T_r-T_e) \tag{21}$$

Power law is assumed for viscosity variation with temperature and ω is exponent in the viscosity law whose value is taken to be 0.76.

Equations (18-21) are applicable for both adiabatic and cooled walls. T_w is wall temperature and is equal to T_r for the case of former and T_c for the latter. All the three examples treated are cooled external flows with recovery factor assumed to be 0.89. Stanton number is evaluated using the Colburn form of the Reynolds analogy[7] which for Prandtl number 0.71 of air becomes

$$St=0.6224\ C_f \tag{22}$$

and is the basis for comparison of local and numerical soltuions in Figs. 2-4.

It is appropriate here to comment upon the step size (x_n-x_{n-1}) used while solving the examples to follow. The values of β for all the examples vary rapidly, as will be seen later, in the region close to the point t. A value of 0.1 in. is therefore used on the blunt portions of wedge and cone and switched over to 0.5 in. on the remaining portions. The step size chosen for the cone is also 0.1 in. close to the point t. However, farther away from t, the step size used is 0.2 in.

Blunt Wedge

Figure 2 shows schematic diagram and the results for a two-dimensional cylindrically blunted wedge. The semiwedge angle is 15° and has a length of 35 in. The radius of cylindrical nose is 3 in. The freestream Mach number is 4 and the freestream stagnation density and temperature are respectively 0.15×10^{-3} lbm/in.[3] and 1600°R. The starting point of turbulent flow is assumed at $x_t=0.7$ in. with θ_t

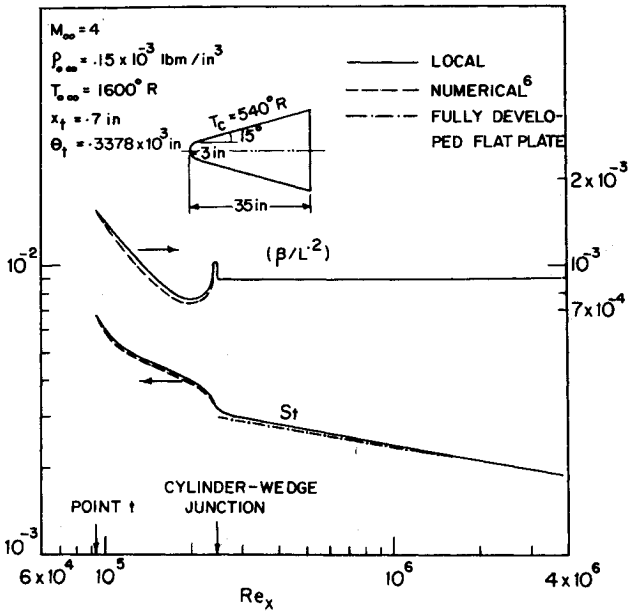

Fig. 2 Schematic diagram and comparison of local, numerical, and fully developed flat plate solutions of a two-dimensional blunt wedge.

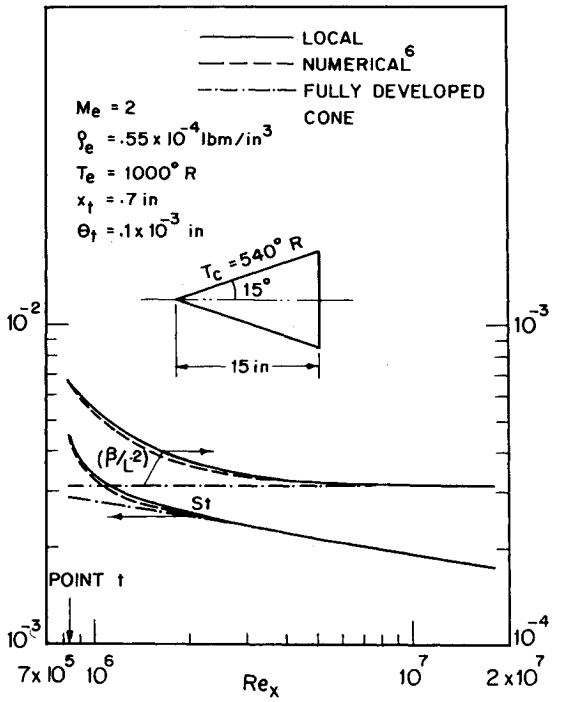

Fig. 3 Schematic diagram and comparison of local, numerical, and fully developed cone solutions.

$= 0.3378 \times 10^{-3}$ in. The wall temperature is assumed as 540°R. The boundary-layer edge conditions are calculated using modified Newtonian theory[8] and isentropic relations.[9]

As can be observed from the figure, the Stanton number calculated from the local analysis deviates slightly from that of the numerical technique. This deviation occurs because the nondimensional $(\beta/L^{0.2})$ (or β), also drawn on the same figure, is not locally constant throughout Re_x, as required by the assumption used in the previous analysis. Based on the Stanton number of the numerical technique, the maximum percentage deviation occurs at $Re_x = 0.126 \times 10^6$ and is 2.5. The deviation, however, is zero at the point t. It is because the Stanton number at the point t is solely determined from Eqs. (2, 3, and 22) which are not affected by the local constancy assumption of β. When Re_x is high, the Stanton number tends

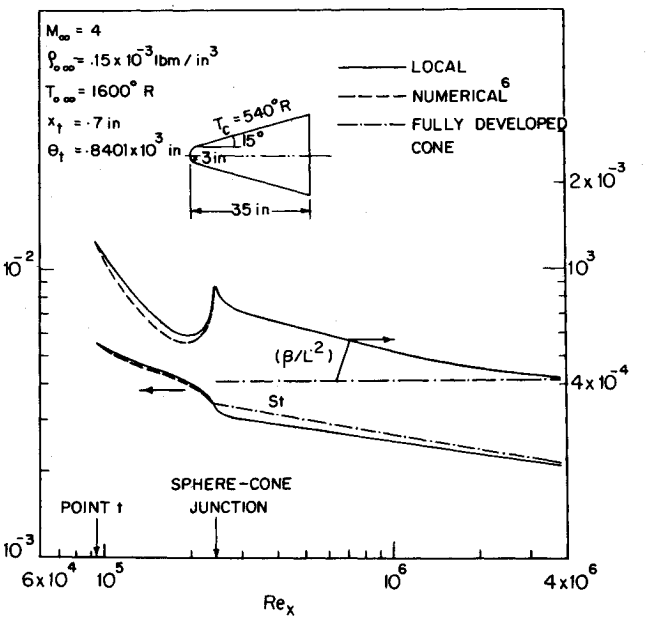

Fig. 4 Schematic diagram and comparison of local, numerical, and fully developed cone solutions of an axisymmetric blunt cone.

asymptotically to that over a fully developed flat plate, Eqs. (15) and (22). This has to be so from both physical and mathematical points of view. For large Re_x (or x), the effects of the bluntness, the starting position of turbulent flow, and the magnitude of momentum thickness at the starting position of turbulent flow becomes insignificant and the flow behaves as a fully turbulent one over a flat plate. Mathematically, this can be explained by observing the behavior of $(\beta/L^{0.2})$ which coincides with the fully developed flat plate value. The magnitude of momentum thickness at cylinder-wedge junction is different, however, from fully developed flat plate flow and delays the attainment by the Stanton number of the flat plate value until Re_x is fairly large.

Cone

Figure 3 shows schematic diagram and the results for a cone. The semiangle is 15° and has a length of 15 in. The flow considered is supersonic with attached shock wave. The flow properties are taken to be $M_e = 2$, $\rho_e = 0.55 \times 10^{-4}$ lbm/in.^{3}, $T_e = 1000°$R, $x_t = 0.7$ in., $\theta_t = 0.1 \times 10^{-3}$ in., and $T_c = 450°$R.

As may be observed from the figure, the Stanton number curves of local analysis and numerical technique are indistinguishable throughout the Re_x range except close to the point t. The maximum percentage deviation occurs at $Re_x = 0.1067 \times 10^7$ and is 2.4%. The difference in the calculated Stanton number is zero at the point t and the explanation given for the blunt wedge example holds here too. For large Reynolds numbers, St tends close to fully developed cone solution, Eqs. (17) and (22). Physically this is expected because, at large distances from the starting point of the turbulent flow, the effects of the starting position of turbulent flow and the magnitude of momentum thickness at the starting point of turbulent flow gets dampened. Mathematically this can be explained by looking at the behavior of $(\beta/L^{0.2})$ drawn on the same figure. It shows that the β of local analysis becomes constant, a condition for the solution to be exact, and is indistinguishable from that of the fully developed cone.

Blunt Cone

Figure 4 shows the schematic diagram and results for blunt cone. The dimensions of the body are the same as of blunt wedge described earlier except that in the present case, the body is an axisymmetric cone with a spherical nose. T_w, M_∞, $\rho_{0\infty}$, $T_{0\infty}$ and x_t have exactly the same values as the blunt

wedge. However the momentum thickness at the transition is different and has a value of 0.8401×10^{-3} in. Modified Newtonian theory and isentropic relations are used to obtain edge conditions.

As may be noted, the Stanton number behavior is similar to that of the blunt wedge and the maximum deviation of the local solution from the numerical solution is 1.8%. The Stanton number tends towards the fully developed cone solution as in the example of the cone discussed earlier when Re_x is large. Physically the explanation is similar to the case of the blunt wedge i.e., the effects of the bluntness, starting position of turbulent flow and the magnitude of momentum thickness at the start of turbulent flow become negligible at large Re_x. Mathematically this is true because, $\beta/L^{0.2}$, drawn on the same figure, is close to that of the fully developed cone value at large Re_x.

Conclusions

An approximate local analytical solution is developed for external or internal compressible turbulent boundary layers. The solution becomes exact for a flat plate with an arbitrary starting point of turbulent flow and for fully developed turbulent cone flow with an attached shock wave. For the numerical examples calculated, the maximum percentage deviation between the local solution and the numerical solution is about 3. Since the solution is a simple analytical one with reasonable accuracy, it can be conveniently used in design of aerospace systems.

Acknowledgment

The author is grateful to R. Narasimha, Department of Aeronautical Engineering, Indian Institute of Science, for several discussions while working on this paper and for technical comments on the prepared manuscript of the paper.

References

[1] Sivells, J. C., "Aerodynamic Design of Axisymmetric Hypersonic Wind Tunnel Nozzles," *Journal of Spacecraft and Rockets*, Vol. 7, Nov. 1970, pp. 1292-1299.

[2] Spence, D. A., "The Growth of Compressible Turbulent Boundary Layers on Isothermal and Adiabatic Walls," Aeronautical Reseach Council, London, R&M No. 3191, 1961.

[3] Reshotko, E. and Tucker, M., "Approximate Calculation of the Compressible Turbulent Boundary Layer with Heat Transfer and Arbitrary Pressure Gradient," NACA TN-4154, 1957.

[4] Bartz, D. R., "An Approximate Solution of Compressible Turbulent Boundary Layer Development and Convective Heat Transfer in Convergent-Divergent Nozzles," *Transactions of the ASME*, Vol. 77, 1955, pp. 1235-1245.

[5] Van Driest, E. R., "Turbulent Boundary Layer on a Cone in a Supersonic Flow at Zero Angle of Attack," *Journal of Aeronautical Sciences*, Vol. 19, 1952, pp. 55-57.

[6] Lakshminarayana, L., "A Fortran-IV Program to Predict Characteristics of Two-Dimensional and Axisymmetric Compressible Turbulent Boundary Layers," Department of Aeronautical Engineering, Indian Institute of Science, Bangalore, Hypersonic Memorandum 14, 1975.

[7] Eckert, E. R. G., "Engineering Relations for Heat Transfer and Friction in High Velocity Laminar and Turbulent Boundary-Layer Flow Over Surfaces with Constant Pressure and Temperature," *Transactions of the ASME*, Vol. 78, June 1956, pp. 1273-1283.

[8] Chernyi, G. G., *Introduction to Hypersonic Flow*, Academic Press, New York and London, 1961, p. 100.

[9] Liepmann, H. W. and Roshko, A., *Elements of Gas Dynamics*, Wiley, New York, 1957, p. 53.